

# Magnetic Field Sensing Beyond the Standard Quantum Limit Using 10-Spin NOON States

Jonathan A. Jones,<sup>1</sup> Steven D. Karlen,<sup>2</sup> Joseph Fitzsimons,<sup>2,3</sup> Arzhang Ardavan,<sup>1</sup> Simon C. Benjamin,<sup>2,4</sup> G. Andrew D. Briggs,<sup>2</sup> John J. L. Morton<sup>1,2,\*</sup>

Quantum entangled states can be very delicate and easily perturbed by their external environment. This sensitivity can be harnessed in measurement technology to create a quantum sensor with a capability of outperforming conventional devices at a fundamental level. We compared the magnetic field sensitivity of a classical (unentangled) system with that of a 10-qubit entangled state, realized by nuclei in a highly symmetric molecule. We observed a 9.4-fold quantum enhancement in the sensitivity to an applied field for the entangled system and show that this spin-based approach can scale favorably as compared with approaches in which qubit loss is prevalent. This result demonstrates a method for practical quantum field sensing technology.

The concept of entanglement, in which coherent quantum states become inextricably correlated (1), has evolved from one of the most startling and controversial outcomes of quantum mechanics to become the enabling principle of emerging technologies such as quantum computation (2) and quantum sensors (3, 4). The use of entangled particles in measurement permits the transcendence of the standard quantum limit in sensitivity, which scales as  $\sqrt{N}$  for  $N$  particles, to the Heisenberg limit, which scales as  $N$ . This approach has been applied to optical interferometry by using entangled photons (5) and by using up to six trapped ions for the measurement of magnetic fields and improvements in atomic clocks (6–8). Spin-squeezing has been investigated as an alternative mode of entanglement generation and has been proposed for sensitive phase detection (9) and demonstrated with four  $^9\text{Be}^+$  ions (10).

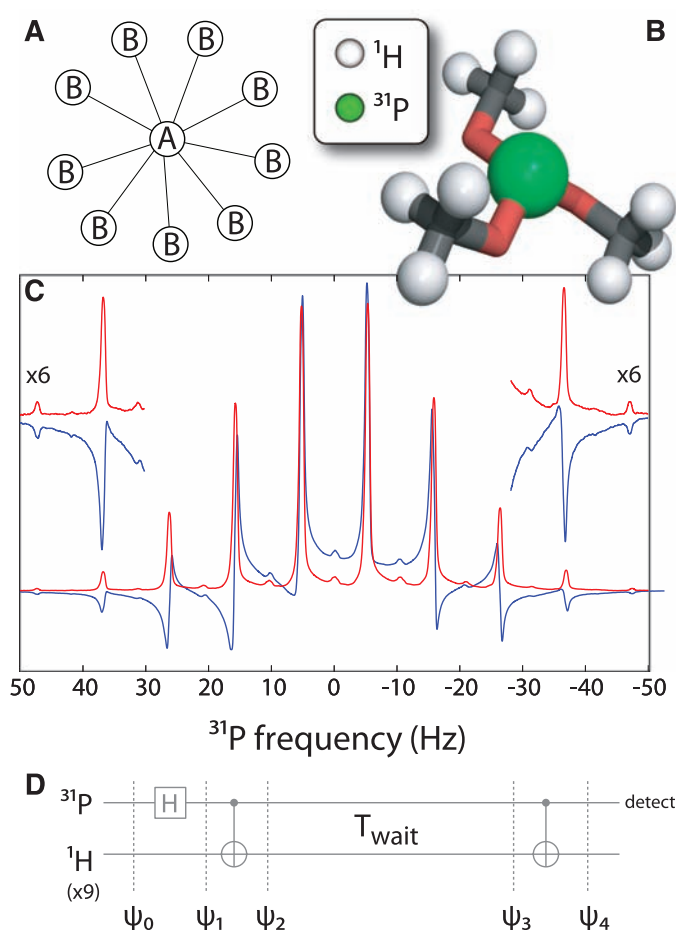
A single spin will precess in the presence of a magnetic field. In the rotating frame used to describe magnetic resonance, this precession occurs at a rate governed by the detuning  $\delta$  of the magnetic field from resonance (expressed in frequency units), so that the state  $|0\rangle + |1\rangle$  evolves as  $|0\rangle + e^{i\delta t}|1\rangle$  (for clarity, normalization constants are omitted throughout). This principle forms the basis of several kinds of magnetic field sensor, in which the externally applied field  $\delta$  is detected as a phase shift. States possessing many-qubit entanglement can acquire phase at a greater rate and thus offer an enhanced sensitivity to the applied field.

<sup>1</sup>Centre for Advanced Electron Spin Resonance (CAESR), Clarendon Laboratory, Oxford University, Oxford OX1 3PU, UK. <sup>2</sup>Department of Materials, Oxford University, Oxford OX1 3PH, UK. <sup>3</sup>Institute of Quantum Computing, University of Waterloo, Waterloo, ON, N2L 3G1, Canada. <sup>4</sup>Centre for Quantum Technologies, National University of Singapore, 3 Science Drive 2, 117543 Singapore.

\*To whom correspondence should be addressed. E-mail: john.morton@materials.ox.ac.uk

The requirements for constructing the resource of a large number of entangled spins are less severe than those for a complete nuclear magnetic resonance (NMR) quantum computer (11–13). Indeed, rather than striving toward individual addressability of each constituent nuclear spin, global addressing is advantageous in quickly and efficiently growing the state. For example, we considered a star topology with

**Fig. 1.** Ten-spin NOON states are created by using nuclear spins in the TMP molecule. **(A)** Topology of the spin qubits used to generate the spin-NOON state. **(B)** The TMP molecule consists of a central  $^{31}\text{P}$  nuclear spin surrounded by nine identical  $^1\text{H}$  spins. **(C)** The initial  $^{31}\text{P}$  NMR spectrum of TMP (red). Nuclear spin-NOON and MSSM states are generated and allowed to evolve for some short time under the influence of an off-resonance magnetic field. After mapping these entangled states back to the  $^{31}\text{P}$ , the resulting spectrum (blue) shows how the phase shift acquired increases with the lopsidedness of the state. Low-intensity peaks between pairs of NMR lines arise from coupling to impurities. **(D)** Spin-NOON states are generated by first applying a Hadamard gate to the  $^{31}\text{P}$  followed by a C-NOT on the nine equivalent  $^1\text{H}$ .



total system depends on a weighted form of  $l$ , which we call  $l_\gamma$ , which includes the relative gyromagnetic ratios of the  $A$  and  $B$  spins. Analogous ideas have been explored in the context of optical Fock states (18).

A molecule with a suitable star topology is trimethyl phosphite (TMP) (Fig. 1B), comprising one central  $^{31}\text{P}$  spin and nine identical surrounding  $^1\text{H}$  spins (the intervening O and C nuclei are mostly spin-zero and may be neglected). The NMR spectrum of  $^{31}\text{P}$  is shown in Fig. 1C (red curve) (19). Coupling to the local  $^1\text{H}$  spins shifts the resonance frequency of the  $^{31}\text{P}$  by some amount depending on the total magnetization of the  $^1\text{H}$ . Within the pseudo-pure state model (11–13), the lines in the  $^{31}\text{P}$  NMR spectrum can thus be assigned to the following  $^1\text{H}$  states:  $|9, 0\rangle, \rho_{8,1}, \rho_{7,2}, \dots, \rho_{1,8}, |0, 9\rangle$ . Any experimentally accessible “many, some” (MS) state is an equal mixture of the relevant pure states  $|M, S\rangle_i$ , where  $i$  runs over the indistinguishable permutations of  $|M, S\rangle$ . We describe MS states in terms of the density matrix  $\rho_{M,S} = \sum_i |M, S\rangle_i \langle M, S|_i$ .

Given the gyromagnetic ratios of  $^1\text{H}$  and  $^{31}\text{P}$  (42.577 and 17.251 MHz/T, respectively), one would predict a  $\sim 23$ -fold enhancement in

phase sensitivity of the 10-spin NOON state over a single  $^{31}\text{P}$  nucleus, or a factor of  $\sim 9.4$  enhancement over the single  $^1\text{H}$  nucleus, which is most commonly used in present sensors.

We now describe the steps required to generate the spin-NOON state and then map the accumulated phase back onto the  $A$  spin (Fig. 1D). The  $A$  spin ( $^{31}\text{P}$ ) in the star topology is distinguishable, and its state is therefore given separately in the spin basis. All the spins start in a ground state:  $\Psi_0 = |0\rangle_A |000 \dots 0\rangle_B = |0\rangle |N, 0\rangle$ . A Hadamard gate is applied to  $A$ , followed by a controlled NOT (C-NOT) gate applied to the  $B$  spins, controlled by the state of  $A$ , yielding  $\Psi_2 = |0\rangle |N, 0\rangle + |1\rangle |0, N\rangle$ : an  $(N+1)$ -spin NOON state with the relevant lopsidedness  $l_\gamma = (N\gamma_B + \gamma_A)/\gamma_B$ . After some period  $T_{\text{wait}}$ ,  $\Psi_3 = |0\rangle |N, 0\rangle + e^{(il_\gamma\delta T_{\text{wait}})} |1\rangle |0, N\rangle$ . A second identical C-NOT is applied to the  $B$  spin in order to map the total phase acquired onto  $A$ :  $\Psi_4 = (|0\rangle + e^{(il_\gamma\delta T_{\text{wait}})} |1\rangle) |N, 0\rangle$ , which is directly detected. A similar C-NOT method has been used to create a  $(1+3)$ -spin entangled state for the purposes of enhanced spin detection (20).

Rather than relying on pseudo-pure-state preparation, we can select to observe the evolution of one of the 10 NMR lines and thus ef-

fectively post-select the signature of a particular initial state, which is analogous to the way in which post-selection has been employed in linear optics experiments on NOON states (5). By applying the entangling operation described above and observing the line corresponding to the original  $B$  ( $^1\text{H}$ ) state  $|9, 0\rangle$ , we can identify the 10-spin NOON state  $|0\rangle |9, 0\rangle + |1\rangle |0, 9\rangle$  and discern its behavior in the presence of a magnetic field detuning  $\delta$ .

Figure 1C (blue curve) shows a measurement of  $^{31}\text{P}$  obtained after the pulse sequence described above and shown in Fig. 1D. The free evolution time  $T_{\text{wait}}$  was set to 400  $\mu\text{s}$  so that given the magnetic field detuning ( $\sim 3.13$   $\mu\text{T}$ ), a phase shift of  $\sim 0.107\pi$  would be experienced by a single  $^1\text{H}$  spin. Observing the left-most line ( $\sim 48$  Hz) is equivalent to post-selecting the  $|0\rangle |9, 0\rangle$  initial state and thus the 10-spin NOON state with  $l_\gamma = 9.4$ , which has instead acquired a  $\sim \pi$  phase shift during the free-evolution period.

An advantage of the mixed initial state of the  $^1\text{H}$  nuclei is that it allows us to simultaneously probe the evolution of all MSSM states for this spin system ( $l_\gamma = |9.4 - 2m|$ , where  $1 \leq m \leq 9$ ). For example, the line at  $\sim 37$  Hz corresponds to the  $\rho_{8,1}$  initial state of the  $B$  spins, which under the operations applied will yield the MSSM state  $\rho_{8,118}$  with  $l_\gamma = 7.4$ , where we define

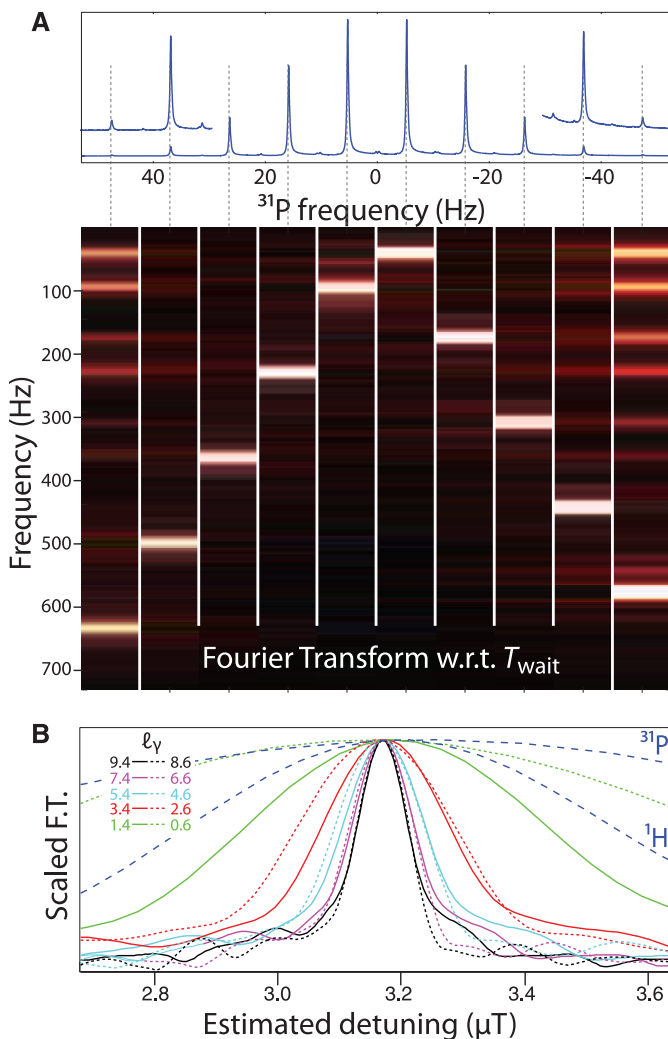
$$\rho_{\text{MSSM}} = \sum_i (|0\rangle |M, S\rangle_i + |1\rangle |S, M\rangle_i) \otimes (\langle 0| \langle M, S|_i + \langle 1| \langle S, M|_i) \quad (1)$$

Each element of the  $\rho_{8,118}$  mixture acquires phase at the same rate, and a phase shift of  $\sim 0.79\pi$  was observed (21). The phase acquired is less than for the ( $l_\gamma = 9.4$ ) state, but the signal-to-noise is greater. Where spin polarization is weak, one of the intermediate MSSM states with  $l < (N+1)$  can yield the optimum sensitivity to magnetic field offset. Moreover, an analysis of the differential phase acquired by successive lines (obtained from a single experiment) can provide more than the single bit of information yielded by one NOON state resource (22).

To explore the evolution of the many-body entangled states in more detail, we varied the evolution time  $T_{\text{wait}}$ . As  $T_{\text{wait}}$  increases, the signal from each line undergoes oscillations whose frequency varies with  $l_\gamma$ . The Fourier transform with respect to  $T_{\text{wait}}$  was measured for the 10 different lines in the  $^{31}\text{P}$  NMR spectrum (Fig. 2). The frequency, which corresponds to a sensitivity to the magnetic field detuning, increases as one moves to the outer lines of the spectrum, corresponding to MSSM states with larger  $l$ , to a maximum for the spin-NOON states at the ends. The linewidth similarly increases slightly because of an enhanced decoherence of the states with larger  $l$ ; however, this increase is sublinear (23), and so when the precession frequency is used to extract an estimate of magnetic field detuning, the uncertainty falls as states with larger  $l$  are used (Fig. 2B).

Our  $|\Psi_{\text{NOON}}\rangle$  is a simple Schrödinger cat state of size  $N = 10$  particles. A state of the form  $\rho_{\text{MSSM}}$  is more complex, but we may say that it is

**Fig. 2.** Nuclear spin-NOON states demonstrate an entanglement-enhanced sensitivity to an external magnetic field. (A) The Fourier transform of the evolution of each of the 10 NMR lines with respect to  $T_{\text{wait}}$  (Fig. 1D) shows an increasing frequency proportional to the increasing lopsidedness  $l_\gamma$  of the entangled state produced. The intensity has been normalized by using the intensities of the initial spectrum; the residual asymmetry in intensities is an artifact of static field inhomogeneity. The  $^{31}\text{P}$  NMR spectrum of the TMP molecule is shown above for reference. (B) The Fourier transform peak allows an estimate of the effective magnetic detuning from resonance of the  $^1\text{H}$  spins, which improves with the use of higher- $l$  states. Solid and dashed lines represent NMR lines to the left and right of center, respectively. Experimental traces that use the unentangled  $^{31}\text{P}$  or  $^1\text{H}$  spins are shown for comparison. All peaks are scaled to unit intensity.



equivalent to a canonical Schrödinger cat state that decoheres at the same rate (24, 25). Then, despite being a mixture,  $\rho_{\text{MSSM}}$  is nevertheless classified as a Schrödinger cat state of full-sized  $N$  within the local decoherence model of (24) (because neither the bit flips nor the mixing inherent in  $\rho_{\text{MSSM}}$  alter the rate at which locally independent phases accumulate). If instead we have global decoherence sources, then the effective Schrödinger cat size will correspond to the lopsidedness  $|M - S|$  for precisely the reasons of field sensitivity described above.

It is worth contrasting the practical utility of the NOON state approach in two scenarios: in which qubit loss is dominant (such as in optical implementations), and in which phase decoherence is dominant (such as in NMR). Losing even a single photon from a NOON state prevents the phase build up from being measured. Other useful photonic states may have greater inherent robustness (18), but such states have yet to be realized experimentally. As the number of photons in the NOON state is increased, the probability of obtaining a successful measurement decreases exponentially. The sensitivity of the NOON state scales only linearly with its size, so the decreasing probability of success rapidly removes any advantage gained through the use of entanglement. For a fixed probability of photon loss  $\epsilon$ , this imposes a fundamental limit, corresponding to the minimum of the dashed curves in Fig. 3. The optimum size of an optical NOON state scales as  $-\log(1 - \epsilon)^{-1}$ , beyond which the use of larger entangled states is detrimental to sensitivity. This practical limitation has motivated the development of alternative methods for optical phase sensing in which neither NOON states, nor indeed entangled states of any kind, are employed (22).

Molecular spin-NOON states do not suffer loss in the same manner as optical systems, and the dominant source of error becomes dephasing noise caused by unaccounted-for fields experienced by individual spins. The effect of such noise versus increasing system size can be characterized by using

an appropriate measurement strategy. In a noise-free system, the rate at which phase  $\phi$  is acquired by the spin-NOON state would correspond directly to the field strength to be detected. We wish to minimize the variance in this quantity (16) so that

$$\Delta^2 \left( \frac{\partial \phi}{\partial t} \right) = \frac{\Delta^2 \phi}{t^2} = \frac{1}{N^2 t^2} \quad (2)$$

Given a fixed time  $T_{\text{tot}}$  to perform the sensor operation, one could make  $M$  separate measurements each of exposure time  $T_E = T_{\text{tot}}/M - T_G$ , where  $T_G$  is the gating and measurement time. This strategy will minimize the effects of finite local noise, provided that  $T_G \ll T_E$ . The variance on the mean of  $M$  individual measurements is

$$\begin{aligned} \Delta^2 \delta &= \frac{1}{M} \left( \frac{1}{N^2 T_E^2} + \frac{1}{N^2} \sum_{i=1}^N \Delta^2 h_i \right) \\ &\approx \frac{1}{T_{\text{tot}}} \left( \frac{1}{N^2 T_E} + \frac{T_E}{N} \Delta^2 h \right) \end{aligned} \quad (3)$$

where  $h_i$  is the phase contribution to spin  $i$  from local fields. For any nonzero  $\Delta^2 h$ , minimizing this quantity will yield  $T_E \propto N^{-1/2}$ , resulting in  $\Delta^2 \phi \propto N^{-3/2}$ . The sensitivity of the system thus limits to  $N^{3/4}$ . Provided that the measurements can be made on a short time scale as compared with the decoherence time of the spin-NOON state ( $\propto N^{-1/2}$ ), creating larger entangled states will produce greater sensitivity.

In addition to demonstrating how an enhanced sensitivity to magnetic fields can be achieved by using entanglement in nuclear spins, this work represents progress toward the realization of “spin amplification” schemes, which use a bath of  $B$  spins to measure the state of  $A$  for the purposes of single-spin detection (20). Analogous to the way in which photon loss poses a limitation to the extent of the resource (photon number), which can be called up for entanglement-enhanced measurement, a weak thermal polarization restricts the effectiveness of

this demonstration for practical magnetometry. Fortunately, the approach described here is readily applicable to electron spins, which can offer a high degree of polarization at experimentally accessible magnetic fields and temperatures. Furthermore, dynamic nuclear polarization, which is already employed in several methods for magnetic field sensing by using nuclear spins (26) or algorithmic cooling (27, 28), could be applied here to yield improvements over currently achievable sensitivity.

References and Notes

1. E. Schrödinger, *Proc. Camb. Philos. Soc.* **31**, 555 (1935).
2. D. Deutsch, *Philos. Trans. R. Soc. London Ser. A* **400**, 97 (1985).
3. B. Yurke, *Phys. Rev. Lett.* **56**, 1515 (1986).
4. V. Giovannetti, S. Lloyd, L. Maccone, *Science* **306**, 1330 (2004).
5. T. Nagata, R. Okamoto, J. L. O'Brien, K. Sasaki, S. Takeuchi, *Science* **316**, 726 (2007).
6. V. Meyer et al., *Phys. Rev. Lett.* **86**, 5870 (2001).
7. C. F. Roos, M. Chwalla, K. Kim, M. Riebe, R. Blatt, *Nature* **443**, 316 (2006).
8. D. Leibfried, M. Barrett, T. Schaetz, J. Britton, *Science* **304**, 1476 (2004).
9. D. Wineland, J. Bollinger, W. Itano, D. Heinzen, *Phys. Rev. A* **50**, 67 (1994).
10. C. Sackett et al., *Nature* **404**, 256 (2000).
11. D. G. Cory, M. D. Price, T. F. Havel, *Physica D* **120**, 82 (1998).
12. N. A. Gershenfeld, I. L. Chuang, *Science* **275**, 350 (1997).
13. J. A. Jones, *Prog. Nucl. Magn. Reson. Spectrosc.* **38**, 325 (2001).
14. B. C. Sanders, *Phys. Rev. A* **40**, 2417 (1989).
15. A. N. Boto et al., *Phys. Rev. Lett.* **85**, 2733 (2000).
16. H. Lee, P. Kok, J. Dowling, *J. Mod. Opt.* **49**, 2325 (2002).
17. E. Knill, R. Laflamme, R. Martinez, C. H. Tseng, *Nature* **404**, 368 (2000).
18. S. D. Huver, C. F. Wildfeuer, J. P. Dowling, *Phys. Rev. A* **78**, 063828 (2008).
19. Materials and methods are available as supporting material on Science Online.
20. P. Cappellaro et al., *Phys. Rev. Lett.* **94**, 020502 (2005).
21. All states of the form  $\rho_{\text{MSSM}}$  (defined in Eq. 1) contain one full ebit of entanglement as described in more detail in (19).
22. B. L. Higgins, D. W. Berry, S. D. Bartlett, H. M. Wiseman, G. J. Pryde, *Nature* **450**, 393 (2007).
23. H. G. Krojanski, D. Suter, *Phys. Rev. Lett.* **93**, 090501 (2004).
24. W. Dür, C. Simon, J. I. Cirac, *Phys. Rev. Lett.* **89**, 210402 (2002).
25. The second approach of (24), based on distillation, does not immediately generalize from their pure states to our mixed states: Under the constraint of single-qubit operations one cannot “produce—with unit probability— $n$ -party [Greenberger-Horne-Zeilinger] states” for  $n > 1$ .
26. N. Kernevez, H. Glénat, *IEEE Trans. Magn.* **27**, 5402 (1991).
27. J. Baugh, O. Moussa, C. A. Ryan, A. Nayak, R. Laflamme, *Nature* **438**, 470 (2005).
28. C. A. Ryan, O. Moussa, J. Baugh, R. Laflamme, *Phys. Rev. Lett.* **100**, 140501 (2008).
29. We thank P. Kok for helpful discussions. This research is supported by the Engineering and Physical Sciences Research Council through the Quantum Information Processing Interdisciplinary Research Collaboration ([www.qipirc.org](http://www.qipirc.org)) (GR/S82176/01) and CAESR (EP/D048559/1). J.F. is supported by Merton College, Oxford. G.A.D.B. is supported by the EPSRC (GR/S15808/01). J.J.L.M. acknowledges St. John’s College, Oxford. J.J.L.M., S.C.B., and A.A. acknowledge support from the Royal Society.

Supporting Online Material

[www.sciencemag.org/cgi/content/full/1170730/DC1](http://www.sciencemag.org/cgi/content/full/1170730/DC1)

Materials and Methods

SOM Text

References

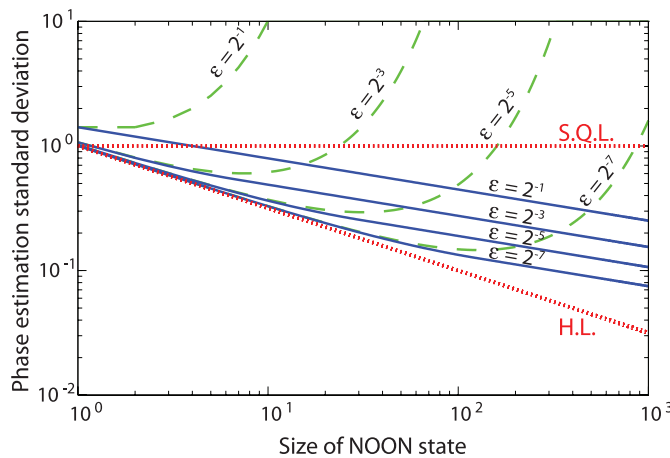
9 January 2009; accepted 25 March 2009

Published online 23 April 2009;

10.1126/science.1170730

Include this information when citing this paper.

**Fig. 3.** Spin-NOON states exhibit an enhanced robustness to noise as compared with optical NOON states. Shown is a comparison of the effect of noise on the SD of phase estimates for spin-NOON (blue solid curves) and optical NOON states (green dashed curves) for a range of error probabilities. For photonic systems, the dominant source of error is taken to be photon loss, which is assumed to occur with probability  $\epsilon$ . For spin-NOON states, the dominant source of error is taken to be a set



of random normally distributed magnetic fields that lead to the complete dephasing of disentangled spins with probability  $\epsilon$  over the time scale of the measurement. The upper and lower dotted lines indicate the standard quantum limit and the Heisenberg limit, respectively. The contribution is plotted per spin/photon, rather than per NOON state, in order to allow a direct comparison of states of varying size.